INTERNATIONAL JOURNAL OF CLIMATOLOGY
Int. J. Climatol. **36**: 2093–2102 (2016)
Published online 14 September 2015 in Wiley Online Library
(wileyonlinelibrary.com) DOI: 10.1002/joc.4486

RMetS
Royal Meteorological Society

Spring Arctic Oscillation-western North Pacific connection in CMIP5 models

Miaoni Gao,[a] Jing Yang,[a]* Daoyi Gong,[a] Haozhe He[a] and Seong-Joong Kim[b]
[a] *State Key Laboratory of Earth Surface Processes and Resource Ecology, Beijing Normal University, China*
[b] *Division of Climate Change, Korea Polar Research Institute, Incheon, South Korea*

ABSTRACT: This study evaluates the simulation of the spring Arctic Oscillation (AO)-western North Pacific linkage based on the 16 state-of-the-art climate models from the Coupled Model Intercomparison Project Phase 5. The validation focuses on the predominant process connecting the spring AO with the East Asian summer monsoon: the formation and persistence of the spring AO-associated cyclonic anomaly over western North Pacific (WPCA) from spring to summer. The results indicate that 8 of 16 models can reproduce both the formation and persistence of the WPCA. Because the formation of the WPCA is directly related to the existence of the spring upper-level North Pacific atmospheric dipole (NPAD), the analyses suggest that a given model can reproduce the spring AO-associated NPAD if the model is capable of simulating the spring AO-associated deceleration of the subtropical westerly jet and the transient eddy activities around the westerly jet exit. Furthermore, the westerly jet anomalies are closely related to the simulated mean state of the westerly jet and the AO Pacific component, which could be further attributed to the simulated sea surface temperature biases over the equatorial Western Pacific.

KEY WORDS spring Arctic Oscillation; western North Pacific; CMIP5; simulation

Received 14 April 2015; Revised 29 June 2015; Accepted 26 July 2015

1. Introduction

The seasonal prediction of the East Asian summer monsoon (EASM) has been a challenging scientific issue due to the distinctive and complex geography of this region (Hsu *et al.*, 2014). The possible precursory signals include the preceding winter/spring tropical Indo-Pacific sea surface temperature (SST) anomalies (e.g. Wang *et al.*, 2000; Xie *et al.*, 2009), spring Atlantic Ocean anomalies (Wu *et al.*, 2009), spring Tibetan Plateau surface thermal conditions (Xu and Li, 2010; Wang *et al.*, 2014) and spring Eurasian continent snow cover (Liu and Yanai, 2002; Yim *et al.*, 2010).

The Arctic Oscillation (AO) has pronounced effects on East Asian climate (e.g. Gong *et al.*, 2002; Yang *et al.*, 2012; Chen *et al.*, 2013; Yun *et al.*, 2014). In terms of mid to high latitudinal preceding signal for the EASM prediction, several previous studies have reported that the spring AO could influence the EASM on an inter-annual timescale by modifying the underlying surface thermal conditions over the Eurasian continent (e.g. Shen and Masahide, 2007) and the north Atlantic SSTs (e.g. Wu *et al.*, 2009). Recently, several studies have shown that the western Pacific local air–sea anomalies imposed by the spring AO play a predominant role on maintaining the spring AO signals through the following summer and consequentially affecting the EASM (Gong *et al.*, 2011; Gao *et al.*, 2013; Chen *et al.*, 2014). According to Gong *et al.* (2011), in the positive phase of the AO, an anomalous cyclone occurs over subtropical North Pacific (between 120°E and 160°W) in the lower troposphere. The anomalous westerly winds of this cyclone decrease the total wind speed over tropical central northern Pacific and warm the tropical ocean surface via the reduced surface evaporation and wind stirring. The warming SST in turn excites ascending atmospheric Rossby waves that reinforce the cyclonic anomaly in their journey to the west from spring to summer. Thus, the anomalous cyclonic circulation over western North Pacific (WNP) maintains to the following summer due to the above-mentioned positive air–sea feedback and leads to the weakened WNP subtropical high (WNPSH) as well as an eastward retreat of the WNPSH, which further weakens the EASM.

The climate model is an indispensable tool to make seasonal predictions. The Coupled Model Intercomparison Project Phase 5 (CMIP5) provides simulation output of current climate models. Several studies have evaluated the models' performances at simulating the EASM (Sperber *et al.*, 2012; Li *et al.*, 2013; Song and Zhou, 2014) and AO (Zhu *et al.*, 2013; Zuo *et al.*, 2013), respectively. However, whether the current climate models can reproduce the spring AO-EASM connection remains unknown, which is one of the key steps to recognize climate models and improve the EASM prediction. Therefore, one of the goals of this study is to investigate this connection in the model simulations with a focus on the WNP processes as above mentioned.

* Correspondence to: J. Yang, State Key Laboratory of Earth Surface Processes and Resource Ecology (ESPRE), Beijing Normal University, No.19 Xinjiekouwai Street, Haidian District, Beijing 100875, China. E-mail: yangjing@bnu.edu.cn

Table 1. Details of the 16 CMIP5 models used in this study.

Model	Institute, country	Resolution (horizontal, vertical) AGCM/OGCM
BNU-ESM	College of Global Change and Earth System Science, Beijing Normal University, China	128 × 64 L26/360 × 200 L50
MPI-ESM-P	Max Planck Institute for Meteorology (MPI-M), Germany	192 × 96 L47/256 × 220 L40
CanESM2	Canadian Centre for Climate Modelling and Analysis, Canada	128 × 64 L35/256 × 192 L40
CESM1-BGC	National Center for Atmospheric Research, America	192 × 288 L26/320 × 384 L60
CESM1-CAM5		192 × 288 L26/320 × 384 L60
CESM1-FASTCHEM		192 × 288 L26/320 × 384 L60
CMCC-CM	Centro Euro-Mediterraneo per I Cambiamenti Climatici, Italy	480 × 240 L31/182 × 149 L31
CNRM-CM5	Centre National de Recherches Meteorologiques/Centre Europeen de Recherche et Formation Avancees en CalculScientifique, France	255 × 128 L31/362 × 292 L42
FGOALS-g2	LASG, Institute of Atmospheric Physics, Chinese Academy of Sciences and CESS, Tsinghua University, China	360 × 180 L26/360 × 196 L30
INMCM4	Institute for Numerical Mathematics, Russia	180 × 120 L21/360 × 340 L40
IPSL-CM5A-LR	Institut Pierre-Simon Laplace, France	96 × 96 L39/182 × 149 L31
HadCM3	Met Office Hadley Centre, United Kingdom	96 × 73 L19/288 × 44 L20
IPSL-CM5B-LR	Institut Pierre-Simon Laplace, France	96 × 96 L39/182 × 149 L31
MIROC-ESM-CHEM	Science and Technology, Atmosphere and Ocean Research Institute (The University of Tokyo), and National Institute for Environmental Studies, Japan	128 × 64 L80/256 × 192 L44
MIROC5	The University of Tokyo, National Institute for Environmental Studies, and Japan Agency for Marine-Earth Science and Technology, Japan	256 × 128 L40/256 × 224 L50
MPI-ESM-LR	Max Planck Institute for Meteorology (MPI-M), Germany	192 × 96 L47/256 × 220 L40

This study aims to address two questions: (1) Are the CMIP5 models able to reproduce the spring AO-WNP connection? (2) What is responsible for the model skills in simulating the spring AO-WNP connection? The remainder of this article is organized as follows. Section 2 presents the data sets, models and methods used in this study. Section 3 describes the spring AO-WNP connection based on observations and the CMIP5 models. Section 4 discusses the possible causes for the different model performances in simulating the spring AO-WNP connection. A summary is provided in Section 5.

2. Data sets, models and methodology

This study is based on the output of the historical experiments of 16 state-of-the-art climate models from CMIP5 (https://pcmdi9.llnl.gov) (Table 1). Each model's result is the average of all experiments' members with equivalent weights. All of the model data are interpolated to a common horizontal grid with a resolution of 2.5° × 2.5°. The monthly and daily data for the period 1979–1997 are used in this study.

The observational data sets we used in this study include (1) the ERA-interim monthly and daily data sets with a 2.5° spatial resolution and 35 pressure levels in the vertical direction produced by the European Centre for Medium-Range Weather Forecasts (Dee *et al.*, 2011) and (2) the SST of Hadley Centre Sea Ice and Sea Surface Temperature data set (HadISST) with a 1° spatial resolution provided by Met Office Hadley Centre (Rayner *et al.*, 2003).

The AO index is the corresponding time coefficients of the first empirical orthogonal function (EOF) of the monthly sea level pressures (SLPs) north of 20°N (Thompson and Wallace, 1998). The spring AO index is the average for March, April and May (MAM). Here, the summer denotes May-June-July (MJJ). The reason for choosing MJJ is that the correlation between Spring AO and WNP is the most significant in this season (Gao *et al.*, 2013). Because we only focus on inter-annual variations, a high-pass filter using a fast Fourier transform is applied to the time series of each variable; only the components with time periods shorter than 8 years remain after the filtering (Bloomfield, 2000); these data are used in the following analysis. The multi-model ensemble (MME) is calculated by averaging the results of each model group using equivalent weights. The atmospheric circulation and SST changes are presented herein as anomalies regressed with the MAM AO index based on both the observation and model outputs.

3. Results

3.1. Observed spring AO-WNP connection

The observed spring AO-associated air–sea characteristics over the WNP from spring to summer are presented in Figure 1. During positive spring AO phases, the lower troposphere over the WNP is dominated by an anomalous cyclone (centring at approximately 180°E, 30°N) in spring (Figure 1(a)). Significant westerly wind anomalies appear over the central tropical North Pacific, north of New Guinea and South China Sea, which suppress the trade

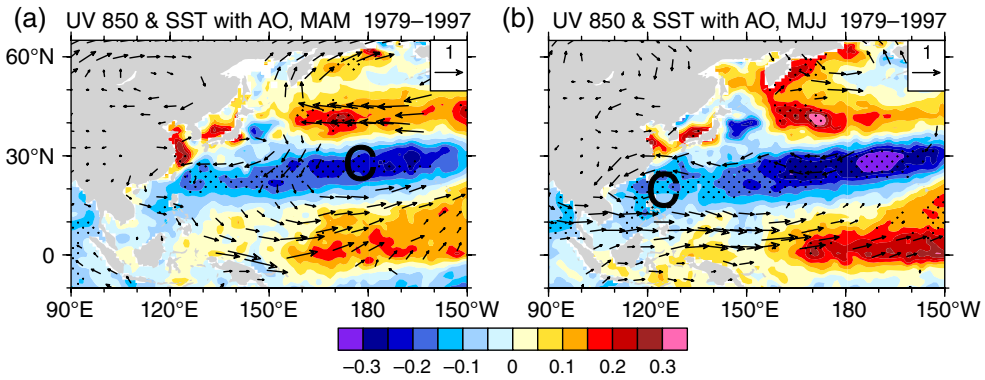

Figure 1. Regressed 850-hPa wind (vectors: m s^{-1}) and SST (shadings: degree) anomalies against the spring AO index based on the ERA-interim reanalysis, respectively, in (a) MAM and (b) MJJ. The areas exceeding the 90% confidence level are dotted, and only the wind vectors that are statistically significant above 90% based on a *t*-test are plotted. 'C' denotes the centre of the cyclonic anomaly.

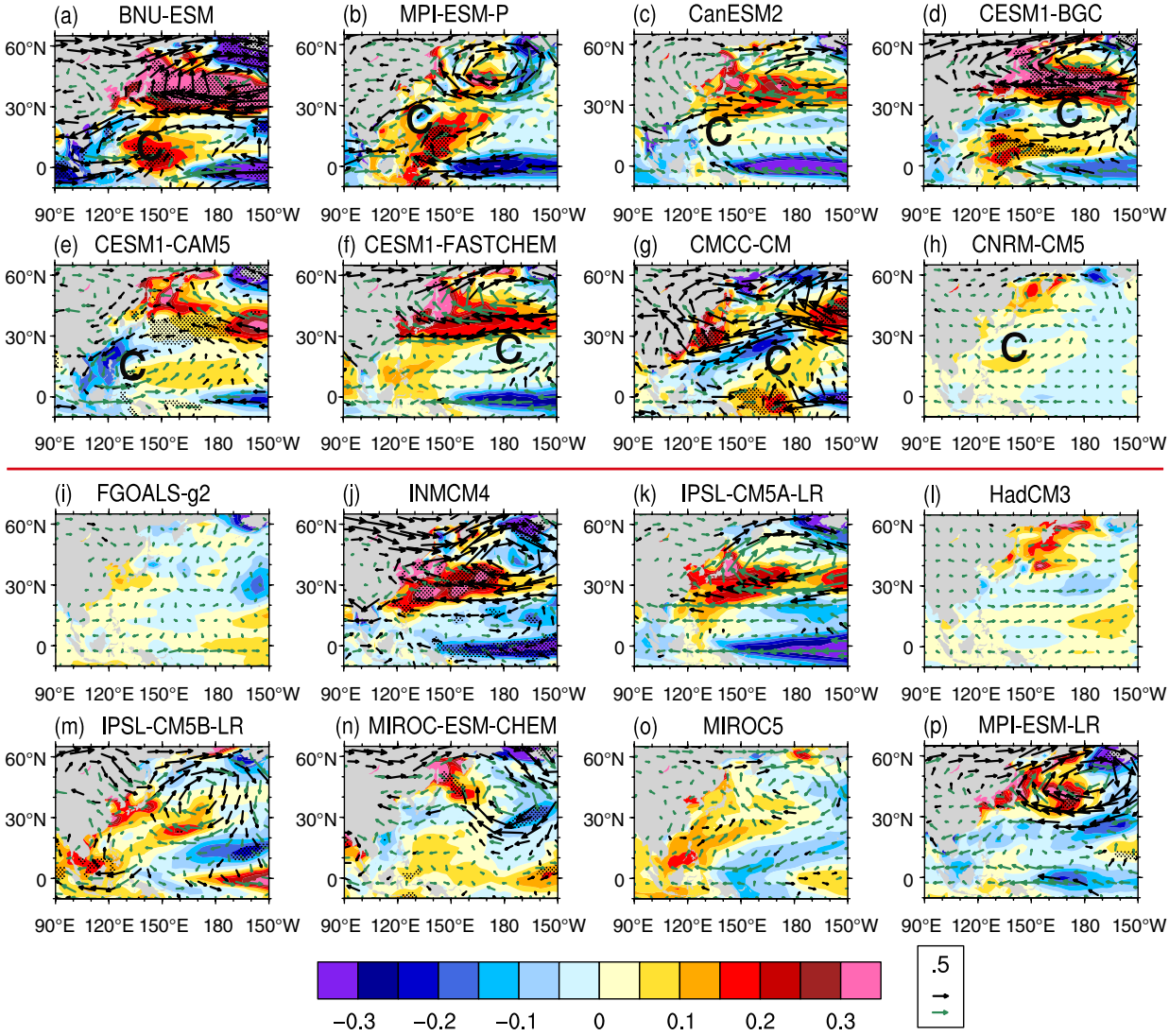

Figure 2. Regressed MAM 850-hPa wind (green and black vectors: m s^{-1}) and SST (shadings: degree) anomalies against the spring AO index for the following models: (a) BNU-ESM, (b) MPI-ESM-P, (c) CanESM2, (d) CESM1-BGC, (e) CESM1-CAM5, (f) CESM1-FASTCHEM, (g) CMCC-CM, (h) CNRM-CM5, (i) FGOALS-g2, (j) INMCM4, (k) IPSL-CM5A-LR, (l) HadCM3, (m) IPSL-CM5B-LR, (n) MIROC-ESM-CHEM, (o) MIROC5 and (p) MPI-ESM-LR. The areas exceeding the 90% confidence level are dotted. The black vectors are statistically significant above 90% based on a *t*-test while the green vectors are not. The red line divides the models into two groups, and 'C' denotes the centre of the cyclonic anomaly.

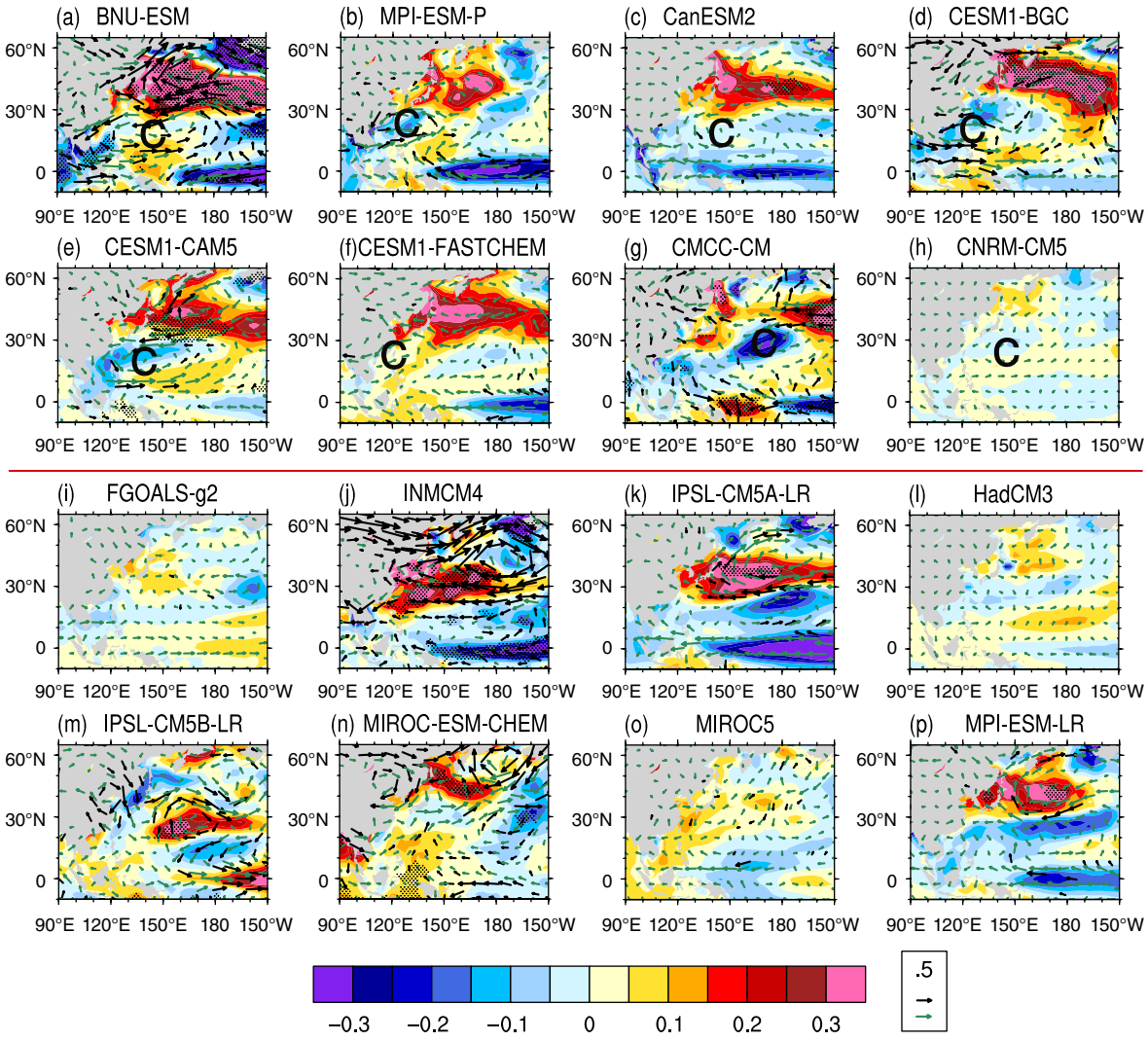

Figure 3. Regressed MJJ 850-hPa wind (green and black vectors: m s^{-1}) and SST (shadings: degree) anomalies against the spring AO index for the following models: (a) BNU-ESM, (b) MPI-ESM-P, (c) CanESM2, (d) CESM1-BGC, (e) CESM1-CAM5, (f) CESM1-FASTCHEM, (g) CMCC-CM, (h) CNRM-CM5, (i) FGOALS-g2, (j) INMCM4, (k) IPSL-CM5A-LR, (l) HadCM3, (m) IPSL-CM5B-LR, (n) MIROC-ESM-CHEM, (o) MIROC5 and (p) MPI-ESM-LR. The areas exceeding the 90% confidence level are dotted. The black vectors are statistically significant above 90% based on a *t*-test while the green vectors are not. The red line divides the models into two groups, and 'C' denotes the centre of the cyclonic anomaly.

winds and increase the local SSTs due to reduced surface evaporation and wind stirring. The increased SSTs in turn excite ascending atmospheric Rossby waves that reinforce the cyclonic anomaly as they propagate westward from spring to summer (Figure 1(b)). Consequently, the spring AO-associated WNP cyclonic anomaly (WPCA) persists from spring to summer and influences the EASM. This evolving process has been addressed in several previous studies (Gill, 1980; Wang *et al.*, 2000; Gong *et al.*, 2011; Gao *et al.*, 2013). Therefore, the WPCA is a crucial component that connects the spring AO with the EASM. However, is the spring AO-associated WPCA that persists from spring to summer reproduced in the CMIP5 models?

3.2. Spring AO-WNP connection in CMIP5 models

To investigate if the models can reproduce the aforementioned spring AO-WNP connection, a regression analysis was performed for the low-level atmospheric circulation and SST anomalies associated with the spring AO from spring to summer based on the output of the 16 CMIP5 models. The results are shown in Figures 2 and 3. First, according to the simultaneous results associated with the spring AO in the simulations, these models can be classified into two categories (Figure 2). There are eight models (BNU-ESM, MPI-ESM-P, CanESM2, CESM1-BGC, CESM1-CAM5, CESM1-FASTCHEM, CMCC-CM and CNRM-CM5) that can roughly reproduce the observed spring WPCA corresponding to the positive spring AO phase (Figure 2(a)–(h)). However, the other eight models (FGOALS-g2, INMCM4, IPSL-CM5A-LR, HadCM3, IPSL-CM5B-LR, MIROC-ESM-CHEM, MIROC5 and MPI-ESM-LR) cannot reproduce the spring AO-associated WPCA (Figure 2(i)–(p)). Hereafter, the first group is called 'WPCA' models, while the second group is called 'non-WPCA' models.

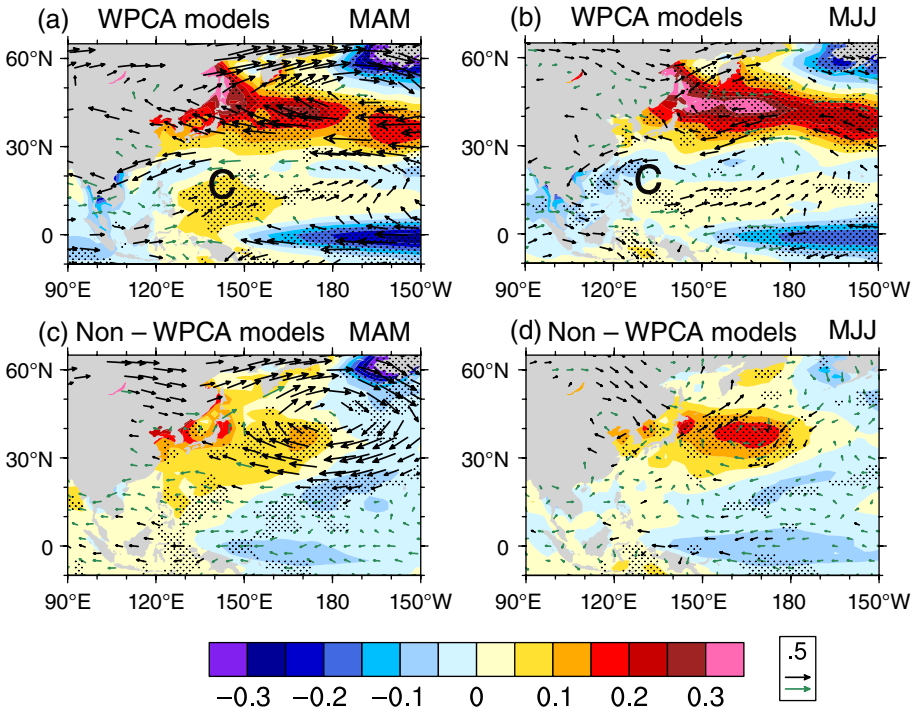

Figure 4. Regressed 850-hPa wind (green and black vectors: m s^{-1}) and SST (shadings: degree) anomalies against the spring AO index for the MME of (a)/(b) the 'WPCA' models and (c)/(d) the 'non-WPCA' models, respectively, and for (a)/(c) MAM and (b)/(d) MJJ. 'C' denotes the centre of the cyclonic anomaly. Dots and black vectors mean that more than 75% models show the same sign responses with the MME on the grids.

We further examined the models' performances in the following summer, respectively, for the two model groups. Generally, the WPCA persists into summer in the eight 'WPCA' models, while no significant WPCA is found in summer in the eight 'non-WPCA' models (Figure 3). To distinguish the differences between the two model groups, the MME was computed for each model group and their evolution from spring to summer were analysed (Figure 4). The simulated WPCA persists from spring to summer in the 'WPCA' models (Figure 4(a) and (b)), and the air–sea features are nearly the same as those depicted in the observations (Figure 1). Consequently, the WPCA weakens the WNPSH and changes the EASM. In contrast, there is no AO-associated circulation pattern over the tropical WNP from spring to summer in the 'non-WPCA' models (Figure 4(c) and (d)). Therefore, an individual model must establish the spring AO-associated WPCA to maintain the spring AO signals through the summer over the East Asia-WNP region.

4. Discussion

In observations, Gong *et al.* (2011) proposed that the formation of the spring AO-associated low-level WPCA is associated with the upper-tropospheric North Pacific atmospheric dipole (NPAD), which consists of an anticyclonic anomaly north of 40°N and a large cyclonic anomaly to the south (Figure 5(a)). And the exit region of the westerly jet core is the axis of this upper-level NPAD. Previous studies have addressed that the interaction between synoptic transient disturbances and the subtropical westerly jet stream

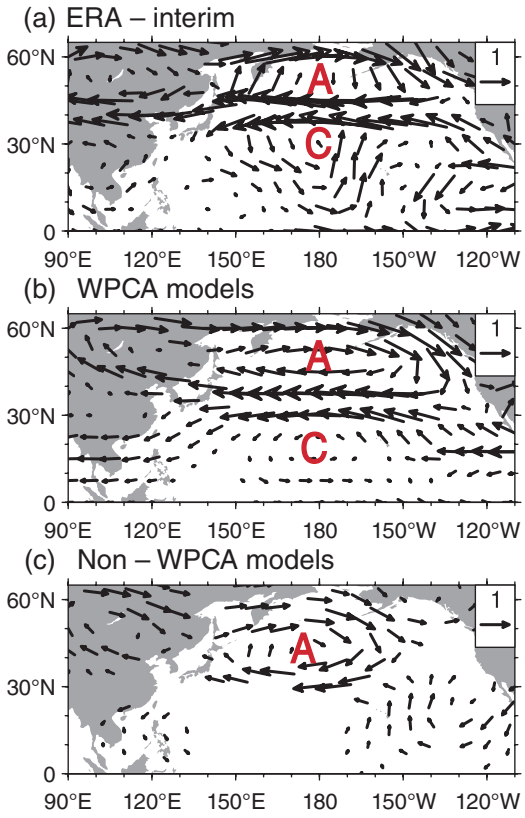

Figure 5. Regressed MAM 300-hPa wind (m s^{-1}) anomalies against the spring AO index for (a) the ERA-interim reanalysis, (b) the MME of the 'WPCA' models and (c) the MME of the 'non-WPCA' models. The 'A' and 'C' denote the centres of the anticyclonic and cyclonic anomalies, respectively. Only the wind vectors that exceed 0.2 m s^{-1} are plotted.

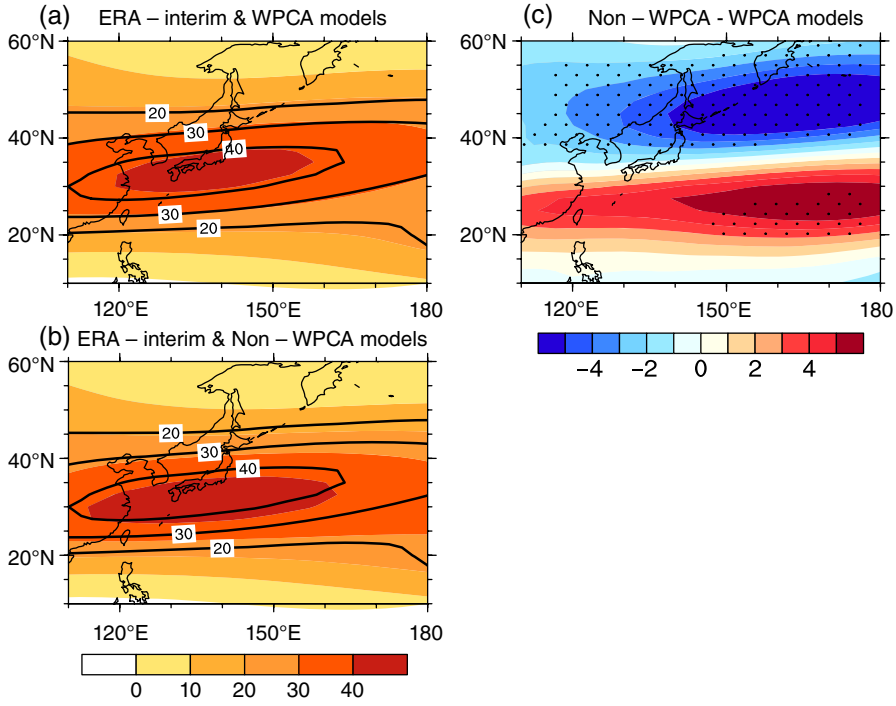

Figure 6. Averaged 200-hPa MAM zonal winds (m s^{-1}) based on the ERA-interim reanalysis (contours), (a) the MME of the 'WPCA' models, (b) the MME of the 'non-WPCA' models (shadings) and (c) the differences between the MME of the 'non-WPCA' models and the MME of the 'WPCA' models ('non-WPCA'-'WPCA'). The areas exceeding 90% confidence level are dotted.

is an important internal source of the monthly mean circulation anomalies, which are important in the formatting of the NPAD (e.g. Lau, 1988; Gong *et al.*, 2011; Chen *et al.*, 2014). Therefore, we hypothesize that the simulated spring AO-associated lower-level WPCA is connected with the upper-level NPAD and that NPAD is related to the mean flow (westerly jet) and transient eddy activities. In the following, we investigate if above hypothesis occur in the two model groups. For brevity, we only show the MME results.

The results show that 'WPCA' models can reproduce the spring AO-associated tropospheric NPAD, although the intensity of its south part is relatively weak (Figure 5(a) and (b)). In contrast, only the northern anticyclonic anomaly of the NPAD is reproduced by the 'non-WPCA' models (Figure 5(c)). This result corresponds to the simulations of the low-tropospheric anomalies (Figure 4(a) and (c)), which is that the WPCA disappears over the lower troposphere in the 'non-WPCA' models. The following question is raised: what influences the models' performances in reproducing the NPAD? Therefore, the subtropical westerly jet stream and transient eddy activities are examined in simulations.

First, the spring subtropical westerly jet core region in the 'WPCA' models better corresponds to the observations than the 'non-WPCA' models, although the jet core shifts slightly southward in the 'WPCA' models relative to the observations (Figure 6(a)). In contrast, the westerly jet core over the WNP is displaced even further southward in the 'non-WPCA' models (Figure 6(b) and (c)). Figure 7(a) shows the differences between the simulated spring SSTs

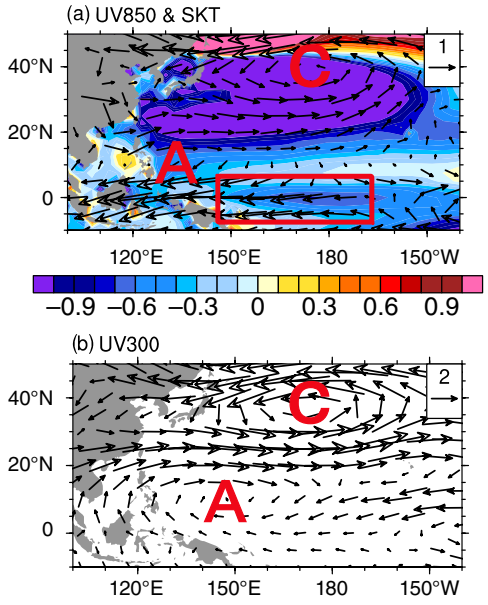

Figure 7. Differences (a) in the simulated 850-hPa winds (vectors: m s^{-1}) and the mean skin temperature (shadings: degrees) and (b) in the simulated 300-hPa winds (vectors: m s^{-1}) between the MME of the 'non- WPCA' models and the MME of the 'WPCA' models in MAM ('non-WPCA'-'WPCA'). The 'A' and 'C' denote the centres of the anticyclonic and cyclonic anomalies, respectively, and the rectangular box indicates the important region.

in two model groups. Compared with the 'WPCA' models, the MAM SSTs have a cold bias over the equatorial western Pacific in the 'non-WPCA' models. This cold SST bias leads to the formation of the simulated anomalous

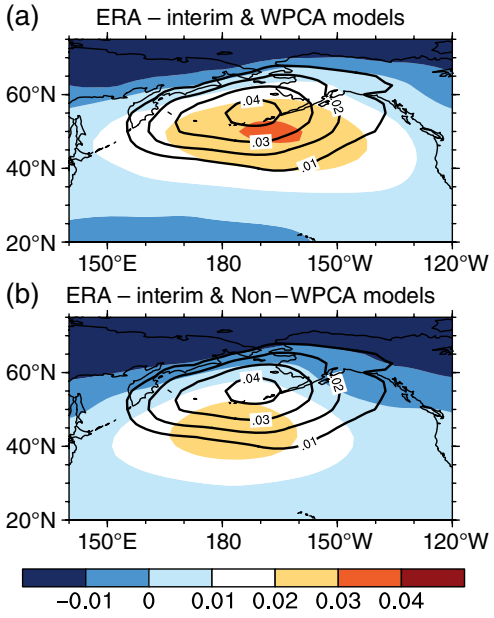

Figure 8. The first leading mode of the MAM sea level pressure (hPa) based on the ERA-interim reanalysis (contours), (a) the MME of the 'WPCA' models and (b) the MME of the 'non-WPCA' models (shadings).

anticyclone over the Philippine Sea by exciting descending atmospheric Rossby waves (Gill, 1980; Wang and Zhang, 2002). The suppressed convection over the Philippine Sea facilitates the generation of the anomalous cyclone east of Japan due to a Pacific-Japan teleconnection (Nitta, 1987; Huang and Lu, 1989; Huang and Sun, 1994). Correspondingly, the westerly anomalies between 20° and 30°N force the subtropical westerly jet southward in the 'non-WPCA' models (Figure 7(b)).

Corresponding to the southward shift of the subtropical westerly jet, the Pacific components of the AO exhibit a pronounced southward displacement in both model groups (Figure 8). Particularly, the AO Pacific anomaly in the 'non-WPCA' models shifts further southward and has a much smaller amplitude than that simulated by the 'WPCA' models (Figure 8(b)). The positive AO weakens the subtropical westerly jet. Therefore, due to the weaker intensity of the AO Pacific component, the spring AO-associated westerly jet deceleration is accordingly smaller in the 'non-WPCA' models than in the 'WPCA' models (Figure 9(b)–(d)), with the 1 m s^{-1} decrease in the velocity of the westerly jet exit. We calculated the standard deviation of 200 hPa zonal winds in the two types of the models (Figure 9(e) and (f)). In 'non-WPCA' models, the standard deviation of 200 hPa zonal winds over the exit of the subtropical westerly jet is 3 m s^{-1} and the contribution from the spring AO is approximately 1 m s^{-1} (Figure 9(c) and (f)). Therefore, the 1 m s^{-1} difference of the spring AO-associated 200 hPa wind anomalies between the two types of models is almost comparable to the AO-induced decrease of westerly jet in 'non-WPCA' models. And the Student *t*-test also exhibits the 1 m s^{-1} difference is statistically significant. Thus, the simulated weaker spring AO-reduced westerly jet may impede the formation of the NPAD in 'non-WPCA' models. This relationship between the AO Pacific component and the WNP atmospheric anomalies has been revealed in previous observational studies (Gao *et al.*, 2013; Chen *et al.*, 2014).

Finally, we examine the role of transient eddies in the simulations. The transient eddy-induced mean circulation can be described by extended Eliassen–Palm (EP) flux (e.g. Hoskins *et al.*, 1983). According to Lau (1988), the EP flux convergence zone is accompanied by negative vorticity to the north and positive vorticity to the south. Thus, the EP flux convergence is associated with an easterly wind acceleration of the mean flow. For ease of calculation, the anomalies of the 200 hPa level extended EP flux (E-vector) is defined as $(\overline{v'^2 - u'^2}, -\overline{u'v'})$, while the eddy kinetic energy is defined as $(\overline{v'^2 + u'^2})$ (Gong *et al.*, 2011). The u' and v' denote the synoptic-scale zonal and meridional winds, respectively, and the overbars represent temporal averages from 1 March through 31 May. Because of data constraints, the MMEs of these 11 models (BNU-ESM, MPI-ESM-P, CanESM2, CMCC-CM, CNRM-CM5, FGOALS-g2, INMCM4, HadCM3, MIROC-ESM-CHEM, MIROC5 and MPI-ESM-LR) are presented in this study. In the observations, the E-vectors convergence zone appears at the exit region of the East Asian jet stream (Figure 10(a)). And the eddy kinetic energy is substantially reduced over the region 150°E–150°W, 35°–50°N, which indicates that the eddy kinetic energy is transformed into low-frequency mean flow. The result suggests that the interaction between mean flow and synoptic-scale eddy plays an important role in generating the spring AO-associated NPAD (Figure 5(a)).

In the 'WPCA' models, the E-vectors convergence zone appears at the exit region of the subtropical westerly jet stream along 180°E and is accompanied by reduced local eddy kinetic energy (Figure 10(b)). Because of the reproducing of the interaction between the eddy kinetic energy and the mean flow, the models are capable of simulating the NPAD. In contrast, the 'non-WPCA' models lack both sufficient E-vectors convergence and decreased synoptic eddy energy over the North Pacific (Figure 10(c)). The differences between two types of the models show that the E-vectors convergence in 'WPCA' models is stronger than that in the 'non-WPCA' models and there are more synoptic eddy energy transforming into the energy of low-frequency mean flow along 180°E in 'non-WPCA' models (Figure 10(d)). The results indicate that the interaction between the eddy kinetic energy and the mean flow is too weak to generate the NPAD in these models. Therefore, realistically simulating synoptic eddy activities near the exit region of the subtropical westerly jet is considered to be important for reproducing the spring AO-associated NPAD in numerical models.

5. Summary

In this study, the spring AO-WNP connection, which is an important process that relates the spring AO with the

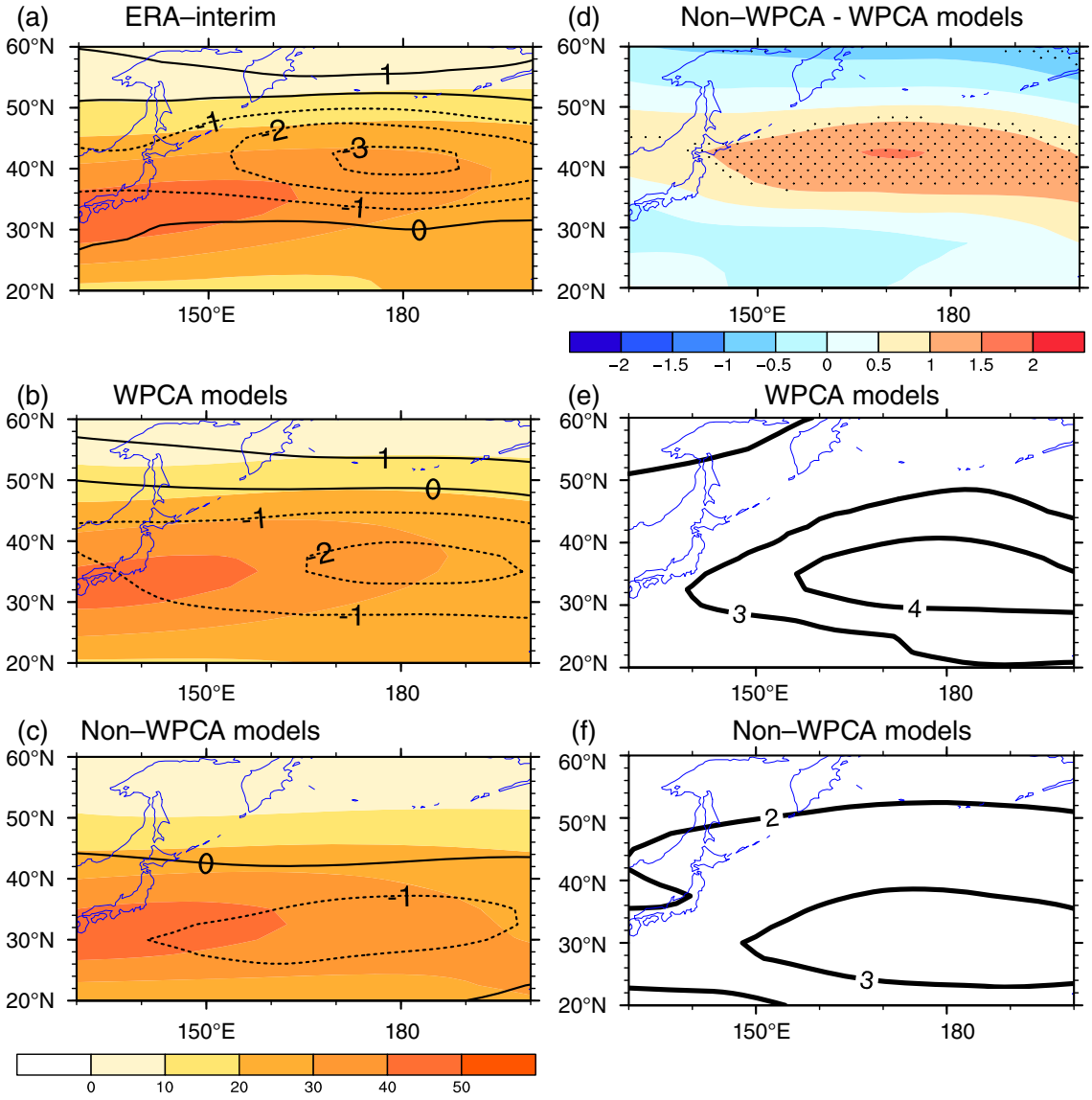

Figure 9. Regressed 200-hPa zonal wind anomalies (contour: m s^{-1}) against the spring AO index and the 200-hPa MAM zonal winds (shadings: m s^{-1}) based on (a) the ERA-interim reanalysis, (b) the MME of the 'WPCA' models, (c) the MME of the 'non-WPCA' models, (d) the difference of the regressed 200-hPa zonal wind anomalies (contour: m s^{-1}) against the spring AO index between 'WPCA' models and 'non-WPCA' models and the standard deviation of the 200-hPa MAM horizontal winds in the (e) 'WPCA' models and (f) 'non-WPCA' models (contours: m s^{-1}). The areas exceeding 90% confidence level are dotted.

EASM, is evaluated based on 16 CMIP5 models. The results indicate that half of the models reproduce this connection, while the other half of the models do not reproduce this connection. Accordingly, the models are categorized into two groups. The first group of models retains the AO signals over the WNP from spring to summer because they reproduce the formation of the spring AO-associated WPCA as well as its persistence through the following summer. The second group of models fails to simulate the spring WPCA so that lose the spring AO signals over the WNP. As a result, it is crucial for a model to reproduce the spring AO-associated WPCA to establish the linkage between the spring AO and the EASM.

Further analyses show that the establishment of the spring WPCA is closely related to the presence of the NPAD. If the spring AO-associated NPAD is reproduced, the spring WPCA also forms in simulations, vice versa. The simulated NPAD may be related to the simulated subtropical westerly jet over the East Asia-WNP and transient eddy activities near the westerly jet exit region. We further speculate that the SST bias over the equatorial Pacific is a potential factor that affects the simulated subtropical westerly jet.

Additionally, the air–sea interaction over the WNP plays an important role in maintaining the WPCA from spring to summer according to previous studies. Therefore, another study is currently being conducted to compare AMIP (Atmospheric Model Intercomparison Project) and CMIP parallel models to verify the role of the WNP air–sea coupling in the connection between the spring AO and the EASM.

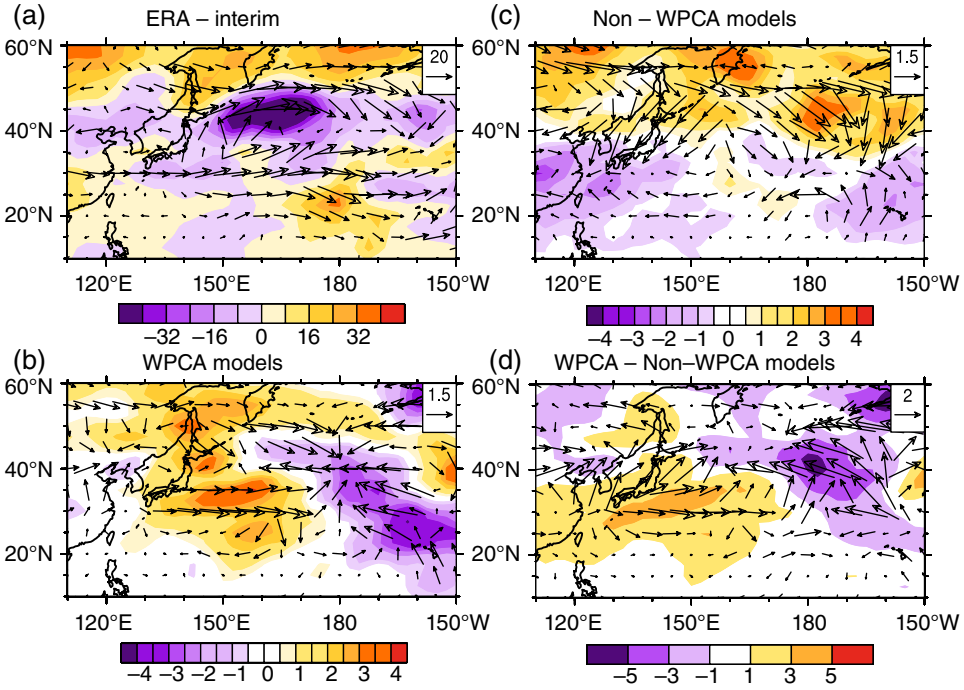

Figure 10. Changes of MAM 200-hPa E-vectors (vector: $m^2\ s^{-2}$) and eddy kinetic energy (shadings: $m^2\ s^{-2}$) in association with the spring AO based on (a) the ERA-interim reanalysis, (b) the MME of the 'WPCA' models, (c) the MME of the 'non-WPCA' models and (d) the difference between two types of models ('WPCA' models – 'non-WPCA' models).

Acknowledgements

This study was supported by National Natural Science Foundation of China (NSFC, grant nos. 41321001 and 41375003), the Beijing Higher Education Young Elite Teacher Project and the project 'Investigation of Climate Change Mechanism by Observation and Simulation of the Polar Climate, Past and Present' (PE15010) of the Korea Polar Research Institute. We are grateful to Dr Ke Wei for providing the datasets used in this study.

References

Bloomfield P. 2000. *Fourier Analysis of Time Series: An Introduction*, 2nd edn. John Wiley & Sons, Inc: Hoboken, NJ.

Chen W, Lan XQ, Wang L, Ma Y. 2013. The combined effects of the ENSO and the Arctic Oscillation on the winter climate anomalies in East Asia. *Chin. Sci. Bull.* **58**: 1355–1362, doi: 10.1007/s11434-012-5654-5.

Chen SF, Yu B, Chen W. 2014. An analysis on the physical process of the influence of AO on ENSO. *Clim. Dyn.* **42**: 973–989, doi: 10.1007/s00382-012-1654-z.

Dee DP, Uppala SM, Simmons AJ, Berrisford P, Poli P, Kobayashi S, Andrae U, Balmaseda MA, Balsamo G, Bauer P, Bechtold P, Beljaars ACM, van de Berg L, Bidlot J, Bormann N, Delsol C, Dragani R, Fuentes M, Geer AJ, Haimberger L, Healy SB, Hersbach H, Hólm EV, Isaksen L, Kållberg P, Köhler M, Matricardi M, McNally AP, Monge-Sanz BM, Morcrette JJ, Park BK, Peubey C, de Rosnay P, Tavolato C, Thépaut JN, Vitart F. 2011. The ERA-Interim reanalysis: configuration and performance of the data assimilation system. *Q. J. R. Meteorol. Soc.* **137**: 553–597, doi: 10.1002/qj.828.

Gao MN, Yang J, Gong DY, Kim SJ. 2013. Unstable relationship between spring Arctic Oscillation and East Asian summer monsoon. *Int. J. Climatol.* **34**(7): 2522–2528, doi: 10.1002/joc.3849.

Gill AE. 1980. Some simple solutions for heat-induced tropical circulation. *Q. J. R. Meteorol. Soc.* **106**: 447–462, doi: 10.1002/qj.49710644905.

Gong DY, Zhu JH, Wang SW. 2002. Significant relationship between spring AO and the summer rainfall along the Yangtze River. *Chin. Sci. Bull.* **47**(11): 948–951, doi: 10.1360/02tb9212.

Gong DY, Yang J, Kim SJ, Gao YQ, Guo D, Zhou TJ, Hu M. 2011. Spring Arctic Oscillation-East Asian summer monsoon connection through circulation changes over the western North Pacific. *Clim. Dyn.* **37**(11-12): 2199–2216, doi: 10.1007/s00382-011-1041-1.

Hoskins BJ, James IN, White GH. 1983. The shape, propagation and mean-flow interaction of large-scale weather systems. *J. Atmos. Sci.* **40**(7): 1595–1612.

Hsu HH, Zhou TJ, Matsumoto J. 2014. East Asian, Indochina and Western North Pacific summer monsoon – an update. *Asia-Pac. J. Atmos. Sci.* **50**(1): 45–68, doi: 10.1007/s13143-014-0027-4.

Huang RH, Lu L. 1989. Numerical simulation of the relationship between the anomaly of the subtropical high over East Asia and the convective activities in the western tropical Pacific. *Adv. Atmos. Sci.* **6**(2): 202–214, doi: 10.1007/BF02658016.

Huang RH, Sun FY. 1994. Impacts of the thermal state and the convective activities in the tropical western warm pool on the summer climate anomalies in East Asia. *Chin. J. Atmos. Sci.* **18**(2): 141–151 (in Chinese).

Lau NC. 1988. Variability of the observed midlatitude storm tracks in relation to low-frequency changes in the circulation pattern. *J. Atmos. Sci.* **45**(19): 2718–2743, doi: 10.1175/1520-0469(1988)045<2718:VOTOMS>2.0.CO;2.

Li RQ, Lv SH, HAN B. 2013. Simulation of Asian-Australian monsoon circulation and variability by 10 CMIP5 models. *J. Trop. Meteorol.* **29**(5): 749–758 (in Chinese).

Liu XD, Yanai M. 2002. Influence of Eurasian spring snow cover on Asian summer rainfall. *Int. J. Climatol.* **22**(9): 1075–1089, doi: 10.1002/joc.784.

Nitta T. 1987. Convective activities in the tropical Western Pacific and their impact on the northern hemisphere summer circulation. *J. Meteorol. Soc. Jpn.* **65**(3): 373–390.

Rayner NA, Parker DE, Horton EB, Folland CK, Alexander LV, Rowell DP, Kent EC, Kaplan A. 2003. Global analyses of sea surface temperature, sea ice and night marine air temperature since the late nineteenth century. *J. Geophys. Res.* **108**(D14): 4407, doi: 10.1029/2002JD002670.

Shen XS, Masahide K. 2007. Studies of the interannual variability of springtime Eurasian surface air temperature. *Chin. J. Atmos. Sci.* **31**: 19–27 (in Chinese).

Song FF, Zhou TJ. 2014. Interannual variability of East Asian summer monsoon simulated by CMIP3 and CMIP5 AGCMs: skill dependence on Indian Ocean-Western Pacific anticyclone teleconnection. *J. Clim.* **27**(4): 1679–1697, doi: 10.1175/JCLI-D-13-00248.1.

Sperber KR, Annamalai H, Kang IS, Kitoh A, Moise A, Turner A, Wang B, Zhou T. 2012. The Asian summer monsoon: an intercomparison of CMIP5 vs. CMIP3 simulations of the late 20th century. *Clim. Dyn.* **41**(9-10): 2711–2744, doi: 10.1007/s00382-012-1607-6.

Thompson DWJ, Wallace JM. 1998. The Arctic Oscillation signature in the wintertime geopotential height and temperature fields. *Geophys. Res. Lett.* **5**: 1297–1300, doi: 10.1029/98GL00950.

Wang B, Zhang Q. 2002. Pacific-East Asian teleconnection, Part II: how the Philippine Sea anticyclone established during development of El Nino. *J. Clim.* **15**(22): 3252–3265, doi: 10.1175/1520-0442(2002)015<3252:PEATPI>2.0.CO;2.

Wang B, Wu RG, Fu XH. 2000. Pacific-East Asia teleconnection: how does ENSO affect East Asian climate? *J. Clim.* **13**: 1517–1536, doi: 10.1175/1520-0442(2000)013<1517:PEATHD>2.0.CO;2.

Wang ZQ, Duan AM, Wu GX. 2014. Time-lagged impact of spring sensible heat over the Tibetan Plateau on the summer rainfall anomaly in East China: case studies using the WRF model. *Clim. Dyn.* **42**(11-12): 2885–2898, doi: 10.1007/s00382-013-1800-2.

Wu ZW, Wang B, Li JP, Jin FF. 2009. An empirical seasonal prediction model of the east Asian summer monsoon using ENSO and NAO. *J. Geophys. Res.* **114**: D18120, doi: 10.1029/2009JD011733.

Xie SP, Hu KM, Hafner J, Tokinaga H, Du Y, Huang G, Sampe T. 2009. Indian Ocean capacitor effect on Indo-Western Pacific climate during the summer following El Niño. *J. Clim.* **22**(3): 730–747, doi: 10.1175/2008JCLI2544.1.

Xu L, Li YQ. 2010. Reexamining the impact of Tibetan snow anomalies to the East Asian summer monsoon using MODIS snow retrieval. *Clim. Dyn.* **35**(6): 1039–1053, doi: 10.1007/s00382-009-0713-6.

Yang J, Gong DY, Wang WS, Hu M, Mao R. 2012. Extreme drought event of 2009/2010 over southwestern China. *Meteorol. Atmos. Phys.* **115**(3-4): 173–184, doi: 10.1007/s00703-011-0172-6.

Yim SY, Jhun JG, Lu RY, Wang B. 2010. Two distinct patterns of spring Eurasian snow cover anomaly and their impacts on the East Asian summer monsoon. *J. Geophys. Res.* **115**: D22113, doi: 10.1029/2010JD013996.

Yun KS, Seo YW, Ha KJ. 2014. Interdecadal changes in the Asian winter monsoon and its relationship with ENSO and AO. *Asia-Pac. J. Atmos. Sci.* **50**(4): 531–540, doi: 10.1007/s13143-014-0042-5.

Zhu X, Dong WJ, Guo Y. 2013. Comparison of simulated winter and spring Arctic Oscillation variability by CMIP5 and CMIP3 coupled models. *Adv. Clim. Change Res.* **9**(3): 165–172, doi: 1673-1719(2013)9:3<165:CJCMSD>2.0.TX;2-X.

Zuo JQ, Li WJ, Ren HL. 2013. Representation of the Arctic Oscillation in the CMIP5 models. *Adv. Clim. Change Res.* **4**(4): 242–249, doi: 10.3724/SP.J.1248.2013.242.

